

Slope parameters determined from CREX and PREX2

Shingo Tagami

Department of Physics, Kyushu University, Fukuoka 819-0395, Japan

Tomotsugu Wakasa

Department of Physics, Kyushu University, Fukuoka 819-0395, Japan

Masanobu Yahiro*

Department of Physics, Kyushu University, Fukuoka 819-0395, Japan

Background: Very lately, the CREX group presents a skin value $\Delta R_{\text{skin}}^{48}(\text{CREX}) = 0.121 \pm 0.026 (\text{exp}) \pm 0.024 (\text{model}) = 0.071 \sim 0.171$ fm. Meanwhile, the PREX group reported a skin value $\Delta R_{\text{skin}}^{208}(\text{PREX2}) = 0.283 \pm 0.071 = 0.212 \sim 0.354$ fm. In our previous paper, we determined both the $L-\Delta R_{\text{skin}}^{48}$ relation and the $L-\Delta R_{\text{skin}}^{208}$ one, using 206 EoSs, where L is a slope parameter.

Purpose: We determine L from $\Delta R_{\text{skin}}^{48}(\text{CREX})$ and $\Delta R_{\text{skin}}^{208}(\text{PREX2})$, using 207 EoSs.

Results: The $\Delta R_{\text{skin}}^{48}(\text{CREX})$ yields $L(\text{CREX}) = 0 \sim 51$ MeV and the $\Delta R_{\text{skin}}^{208}(\text{PREX2})$ does $L(\text{PREX2}) = 76 \sim 165$ MeV.

Conclusion: There is no overlap between $L(\text{CREX})$ and $L(\text{PREX2})$. This is a big problem to be solved.

I. INTRODUCTION AND CONCLUSION

Background on experiments:

Horowitz, Pollock and Souder proposed a direct measurement for neutron skin thickness $\Delta R_{\text{skin}} = r_n - r_p$ [1], where r_p and r_n are proton and neutron radii, respectively. This direct measurement consists of parity-violating and elastic electron scattering. In fact, the PREX collaboration has reported a new value,

$$\Delta R_{\text{skin}}^{208}(\text{PREX2}) = 0.283 \pm 0.071 = 0.212 \sim 0.354 \text{ fm}, \quad (1)$$

combining the original Lead Radius EXperiment (PREX) result [2, 3] with the updated PREX2 result [4]. For ^{48}Ca , the CREX group presents [5]

$$\begin{aligned} \Delta R_{\text{skin}}^{48}(\text{CREX}) &= 0.121 \pm 0.026 (\text{exp}) \pm 0.024 (\text{model}) \\ &= 0.071 \sim 0.171 \text{ fm}. \end{aligned} \quad (2)$$

Note that the direct values are obtained from a single momentum transfer q . As an *ab initio* method for ^{48}Ca , we should consider the coupled-cluster (CC) method [6, 7] with chiral interaction. The CC result $\Delta R_{\text{skin}}^{48}(\text{CC}) = 0.12 \sim 0.15$ fm [7] is consistent with $\Delta R_{\text{skin}}^{48}(\text{CREX})$.

As an indirect measurement on ΔR_{skin} , the high-resolution $E1$ polarizability experiment ($E1pE$) was made for ^{208}Pb [8] and ^{48}Ca [9] in RCNP. The results are

$$\Delta R_{\text{skin}}^{208}(E1pE) = 0.156_{-0.021}^{+0.025} = 0.135 \sim 0.181 \text{ fm}, \quad (3)$$

$$\Delta R_{\text{skin}}^{48}(E1pE) = 0.14 \sim 0.20 \text{ fm}. \quad (4)$$

The $\Delta R_{\text{skin}}^{48}(\text{CREX})$ is consistent with $\Delta R_{\text{skin}}^{48}(E1pE)$, but $\Delta R_{\text{skin}}^{208}(\text{PREX2})$ is not with $\Delta R_{\text{skin}}^{208}(E1pE)$.

Reaction cross section σ_R is a standard observable to determine the matter radius r_m and the skin value ΔR_{skin} . High-accuracy data $\sigma_R(\text{exp})$ are available for $^{42-51}\text{Ca} + ^{12}\text{C}$ scattering at 280 MeV per nucleon [10]. The chiral (Kyushu) g -matrix folding model [11] yields $\Delta R_{\text{skin}}^{48}(\text{exp}) = 0.105 \pm 0.06$ fm from the data [12]. The result is consistent with $\Delta R_{\text{skin}}^{48}(\text{CREX})$. High-accuracy data $\sigma_R(\text{exp})$ are available also for $p + ^{208}\text{Pb}$ scattering in $21 \leq E_{\text{lab}} \leq 180$ MeV [13–15]. The chiral (Kyushu) g -matrix folding model yields $\Delta R_{\text{skin}}^{208}(\text{exp}) = 0.278 \pm 0.035$ fm [16]. The value is consistent with $\Delta R_{\text{skin}}^{208}(\text{PREX2})$.

Matter:

Among the basic physical quantities that determine the equation of state (EoS) of nuclear systems, the symmetry energy (S_{sym}) and its dependence on the nucleon density (ρ) are receiving a lot of attention, because of their critical role in shaping the structure of nuclei and neutron stars (NSs) [17–23]. Many predictions on the symmetry energy $S_{\text{sym}}(\rho)$ have been made so far by taking several experimental and observational constraints on $S_{\text{sym}}(\rho)$ and their combinations. The $\Delta R_{\text{skin}}^{208}(E1pE)$ and the $\Delta R_{\text{skin}}^{48}(\text{CREX})$ are the most important experimental constraint on the slope parameter L , since a strong correlation between r_{skin}^{208} and L is well known [24, 25]. In this paper, we will show a strong correlation between r_{skin}^{48} and L and between r_{skin}^{208} and L from 207 EoSs.

As an essential constraint on the EoS from astrophysics, one may take $M = 1.97 \pm 0.04 M_{\text{sun}}$ [26], where M is the mass of NS. For a pulsar in a binary system, detection of the general relativistic Shapiro delay allows us to determine M .

Usually, the S_{sym} is expanded into

$$S_{\text{sym}}(\rho) = J + \frac{L(\rho - \rho_0)}{3\rho_0} + \frac{K_{\text{sym}}(\rho - \rho_0)^2}{18\rho_0^2} + \dots \quad (5)$$

in terms of the nuclear density ρ around the saturation density ρ_0 . For the $S_{\text{sym}}(\rho)$, at the present stage, a major aim is to determine L at $\rho = \rho_0$. The symmetry energy $S_{\text{sym}}(\rho)$ cannot be measured by experiment directly. In place of $S_{\text{sym}}(\rho)$, the

* orion093g@gmail.com

neutron-skin thickness r_{skin} is measured to determine L . This subject is currently under experimental investigation for ^{208}Pb and ^{48}Ca nuclei at Jefferson Lab [27–29].

Figure 1 shows the binding energy per nucleon E/A as a function of ρ and $\delta = (N - Z)/A$. The E/A is expanded into

$$\frac{E(\rho, \delta)}{A} = S_0(\rho) + S_{\text{sym}}(\rho)\delta^2 + \dots \quad (6)$$

in terms of δ ; note that $J = S_0(\rho_0)$. This equation shows the relation between $E/A(\rho, \delta)$ and $S_{\text{sym}}(\rho)$. Two curves correspond to the symmetric-nuclear matter with $\delta = 0$ and pure-neutron matter with $\delta = 1$, respectively. This figure shows that L is a slope for pure-neutron matter at $\rho = \rho_0$, because $dS_0(\rho)/d\rho$ is zero at $\rho = \rho_0$.

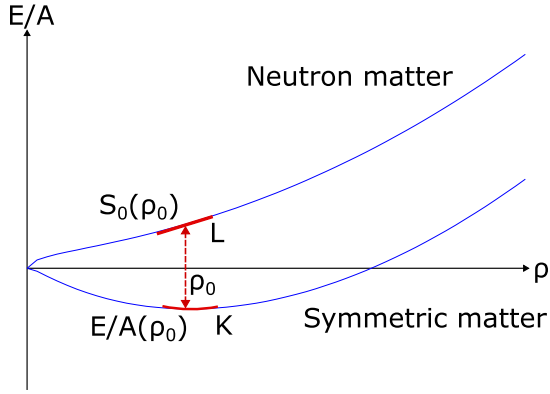


FIG. 1. Illustration on the physics meaning of the slope parameter L and the incompressibility K .

We accumulate the 205 EoSs from Refs. [20, 24, 30–55] in which $\Delta R_{\text{skin}}^{208}$ and/or L is presented, since a strong correlation between $\Delta R_{\text{skin}}^{208}$ and a slope parameter L is shown. In the 205 EoSs of Table I, the number of Gogny EoSs is much smaller than that of Skyrme EoSs. In Ref. [56], we constructed DIMK and DIPK. Eventually, we get the 207 EoSs, as shown in Table I. The correlation is more reliable when the number of EoSs is larger. For this reason, we take the 207 EoSs.

Among the 207 EoSs, APR of Ref. [30] is the most reliable EoS, since they calculated properties of dense symmetric-nuclear and pure-nuclear matter and the structure of neutron stars with the variational chain summation methods for the Argonne v18 two-nucleon interaction plus the Urbana three nucleon interaction. The methods are hard to calculate. In fact, Steiner *et al.* have fit bulk properties of APR for symmetric-nuclear and neutron matter with a Skyrme-like Hamiltonian [40]. The EoS is called NRAPR. Brown and Schwenk modified NRAPR slightly [43]. The EoS is called NRAPR-B in this paper. Tsang *et al.* made further modification for NRAPR-B [46]. The EoS is called NRAPR-T in this paper.

The $\Delta R_{\text{skin}}^{208}$ (PREX2) and $\Delta R_{\text{skin}}^{48}$ (CREX) is most reliable, and provides L of nuclear matter. In fact, using 207 EoSs of Table I, we found the L - $\Delta R_{\text{skin}}^{48}$ relation [56] as

$$\Delta R_{\text{skin}}^{48} = 0.0009L + 0.125 > 0.125 \text{ fm} \quad (7)$$

with a high correlation coefficient $R = 0.98$, because of $L > 0$. Equation (7) indicates that the lower limit of $\Delta R_{\text{skin}}^{48}$ is 0.125 fm. The same derivation is possible the L - $\Delta R_{\text{skin}}^{208}$ relation:

$$L = 620.39 \Delta R_{\text{skin}}^{208} - 57.963 \quad (8)$$

has $R = 0.99$. The two relations are visualized by Fig. 2.

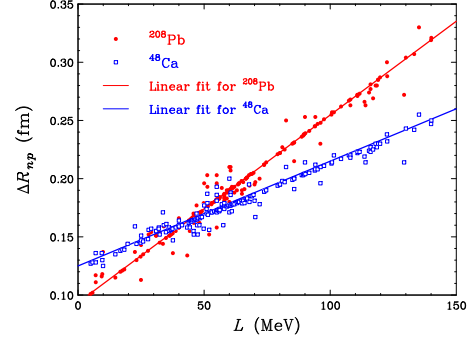


FIG. 2. Skin value ΔR as a function of L for ^{208}Pb and ^{48}Ca . Two straight line show Eq. (7) and Eq. (8), respectively. Dots denote 207 EoSs for ^{208}Pb and ^{48}Ca .

Results: Figure 3 shows the relation between $\Delta R_{\text{skin}}^{208}$ and $\Delta R_{\text{skin}}^{48}$. The 207 EoSs do not satisfy both $\Delta R_{\text{skin}}^{208}$ (PREX2) and $\Delta R_{\text{skin}}^{48}$ (CREX) in the one- σ level. If one considers the two- σ level of $\Delta R_{\text{skin}}^{208}$ (PREX2) and $\Delta R_{\text{skin}}^{48}$ (CREX), one may find that some EoSs satisfy $\Delta R_{\text{skin}}^{208}$ (PREX2) and $\Delta R_{\text{skin}}^{48}$ (CREX)

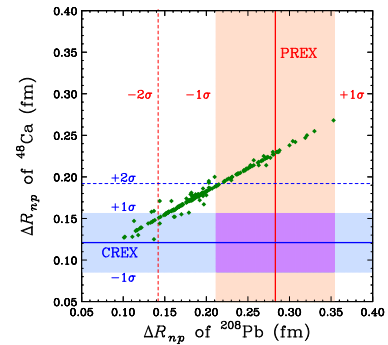


FIG. 3. Relation between $\Delta R_{\text{skin}}^{208}$ and $\Delta R_{\text{skin}}^{48}$.

The L - $\Delta R_{\text{skin}}^{48}$ relation of Eq. (7) yields $L(\text{CREX}) = 0 \sim 51 \text{ MeV}$ and the L - $\Delta R_{\text{skin}}^{208}$ of Eq. (8) does $L(\text{PREX2}) =$

76 \sim 165 MeV. There is no overlap between them. Note that the value of L should be positive. The later value is consistent with $L = 76 \sim 172$ MeV of Ref. [24]. Reed *et al.* [57] report a value of the slope parameter $L = 106 \pm 37 = 69 \sim 143$ MeV.

Conclusion: There is no overlap between $L(\text{CREX})$ and $L(\text{PREX2})$ in the one- σ level, as shown in Fig. 3. This is

a big problem to be solved. As another problem, we can say that APR [30, 31, 44] as the most reliable EoS is ruled out.

ACKNOWLEDGEMENTS

We thank Prof. Matsuzaki for his comments.

-
- [1] C. J. Horowitz, S. J. Pollock, P. A. Souder, and R. Michaels, Phys. Rev. C **63**, 025501 (2001).
- [2] S. Abrahamyan, Z. Ahmed, H. Albatineh, K. Aniol, D. S. Armstrong, W. Armstrong, T. Averett, B. Babineau, A. Barbieri, V. Bellini, *et al.* (PREX Collaboration), Phys. Rev. Lett. **108**, 112502 (2012).
- [3] C. J. Horowitz, Z. Ahmed, C.-M. Jen, A. Rakhman, P. A. Souder, M. M. Dalton, N. Liyanage, K. D. Paschke, K. Saenboonruang, R. Silwal, G. B. Franklin, M. Friend, B. Quinn, K. S. Kumar, D. McNulty, L. Mercado, S. Riordan, J. Wexler, R. W. Michaels, and G. M. Urciuoli, Phys. Rev. C **85**, 032501 (2012).
- [4] D. Adhikari *et al.* (PREX), Phys. Rev. Lett. **126**, 172502 (2021), arXiv:2102.10767 [nucl-ex].
- [5] D. Adhikari *et al.* (CREX), Phys. Rev. Lett. **129**, 042501 (2022), arXiv:2205.11593 [nucl-ex].
- [6] G. Hagen, T. Papenbrock, M. Hjorth-Jensen, and D. J. Dean, Rept. Prog. Phys. **77**, 096302 (2014), arXiv:1312.7872 [nucl-th].
- [7] G. Hagen *et al.*, Nature Phys. **12**, 186 (2015), arXiv:1509.07169 [nucl-th].
- [8] A. Tamii *et al.*, Phys. Rev. Lett. **107**, 062502 (2011), arXiv:1104.5431 [nucl-ex].
- [9] J. Birkhan *et al.*, Phys. Rev. Lett. **118**, 252501 (2017), arXiv:1611.07072 [nucl-ex].
- [10] M. Tanaka *et al.*, Phys. Rev. Lett. **124**, 102501 (2020), arXiv:1911.05262 [nucl-ex].
- [11] M. Toyokawa, M. Yahiro, T. Matsumoto, and M. Kohno, PTEP **2018**, 023D03 (2018), arXiv:1712.07033 [nucl-th].
- [12] M. Takechi, T. Wakasa, S. Tagami, J. Matsui, and M. Yahiro, Results Phys. **31**, 104923 (2021), arXiv:2009.00796 [nucl-th].
- [13] R. F. Carlson, A. J. Cox, J. R. Nimmo, N. E. Davison, S. A. Elbaker, J. L. Horton, A. Houdayer, A. M. Sourkes, W. T. H. van Oers, and D. J. Margaziotis, Phys. Rev. C **12**, 1167 (1975).
- [14] A. Ingemarsson, J. Nyberg, P. Renberg, O. Sundberg, R. Carlson, A. Auce, R. Johansson, G. Tibell, B. Clark, L. Kurth Kerr, and S. Hama, Nucl. Phys. A **653**, 341 (1999).
- [15] A. Auce, A. Ingemarsson, R. Johansson, M. Lantz, G. Tibell, R. F. Carlson, M. J. Shachno, A. A. Cowley, G. C. Hillhouse, N. M. Jacobs, *et al.*, Phys. Rev. C **71**, 064606 (2005).
- [16] S. Tagami, T. Wakasa, J. Matsui, M. Yahiro, and M. Takechi, Phys. Rev. C **104**, 024606 (2021), arXiv:2010.02450 [nucl-th].
- [17] C. J. Horowitz and J. Piekarewicz, Phys. Rev. Lett. **86**, 5647 (2001), arXiv:astro-ph/0010227.
- [18] J. M. Lattimer and A. W. Steiner, Eur. Phys. J. A **50**, 40 (2014), arXiv:1403.1186 [nucl-th].
- [19] M. Baldo and G. F. Burgio, Prog. Part. Nucl. Phys. **91**, 203 (2016), arXiv:1606.08838 [nucl-th].
- [20] M. Oertel, M. Hempel, T. Klähn, and S. Typel, Rev. Mod. Phys. **89**, 015007 (2017), arXiv:1610.03361 [astro-ph.HE].
- [21] J. Piekarewicz and F. J. Fattoyev, (2019), 10.1063/PT.3.4247, arXiv:1907.02561 [nucl-th].
- [22] Y. Zhang, M. Liu, C.-J. Xia, Z. Li, and S. K. Biswal, Phys. Rev. C **101**, 034303 (2020), arXiv:2002.10884 [nucl-th].
- [23] G. F. Burgio, H. J. Schulze, I. Vidana, and J. B. Wei, Prog. Part. Nucl. Phys. **120**, 103879 (2021), arXiv:2105.03747 [nucl-th].
- [24] X. Roca-Maza, M. Centelles, X. Vinas, and M. Warda, Phys. Rev. Lett. **106**, 252501 (2011), arXiv:1103.1762 [nucl-th].
- [25] B. A. Brown, Phys. Rev. Lett. **111**, 232502 (2013), arXiv:1308.3664 [nucl-th].
- [26] P. Demorest, T. Pennucci, S. Ransom, M. Roberts, and J. Hessels, Nature **467**, 1081 (2010), arXiv:1010.5788 [astro-ph.HE].
- [27] S. Abrahamyan *et al.*, Phys. Rev. Lett. **108**, 112502 (2012), arXiv:1201.2568 [nucl-ex].
- [28] S. Tagami, N. Yasutake, M. Fukuda, and M. Yahiro, (2020), arXiv:2003.06168 [nucl-th].
- [29] D. Adhikari *et al.* (PREX), Phys. Rev. Lett. **126**, 172502 (2021), arXiv:2102.10767 [nucl-ex].
- [30] A. Akmal, V. R. Pandharipande, and D. G. Ravenhall, Phys. Rev. C **58**, 1804 (1998), arXiv:nucl-th/9804027.
- [31] C. Ishizuka, T. Suda, H. Suzuki, A. Ohnishi, K. Sumiyoshi, and H. Toki, Publ. Astron. Soc. Jap. **67**, 13 (2015), arXiv:1408.6230 [nucl-th].
- [32] C. Gonzalez-Boquera, M. Centelles, X. Viñas, and L. M. Robledo, Phys. Lett. B **779**, 195 (2018), arXiv:1712.06735 [nucl-th].
- [33] M. Farine, D. Von-Eiff, P. Schuck, J. F. Berger, J. Dechargé, and M. Girod, **25**, 863 (1999).
- [34] C. Gonzalez-Boquera, M. Centelles, X. Viñas, and A. Rios, Phys. Rev. C **96**, 065806 (2017), arXiv:1706.02736 [nucl-th].
- [35] J. Piekarewicz, Phys. Rev. C **76**, 064310 (2007), arXiv:0709.2699 [nucl-th].
- [36] Y. Lim, K. Kwak, C. H. Hyun, and C.-H. Lee, Phys. Rev. C **89**, 055804 (2014), arXiv:1312.2640 [nucl-th].
- [37] R. Sellaheewa and A. Rios, Phys. Rev. C **90**, 054327 (2014), arXiv:1407.8138 [nucl-th].
- [38] T. Inakura and H. Nakada, Phys. Rev. C **92**, 064302 (2015), arXiv:1509.02982 [nucl-th].
- [39] F. J. Fattoyev and J. Piekarewicz, Phys. Rev. Lett. **111**, 162501 (2013), arXiv:1306.6034 [nucl-th].
- [40] A. W. Steiner, M. Prakash, J. M. Lattimer, and P. J. Ellis, Phys. Rept. **411**, 325 (2005), arXiv:nucl-th/0410066.
- [41] M. Centelles, X. Roca-Maza, X. Vinas, and M. Warda, Phys. Rev. C **82**, 054314 (2010), arXiv:1010.5396 [nucl-th].
- [42] M. Dutra, O. Lourenco, J. S. Sa Martins, A. Delfino, J. R. Stone, and P. D. Stevenson, Phys. Rev. C **85**, 035201 (2012), arXiv:1202.3902 [nucl-th].
- [43] B. A. Brown and A. Schwenk, Phys. Rev. C **89**, 011307 (2014), [Erratum: Phys.Rev.C 91, 049902 (2015)], arXiv:1311.3957 [nucl-th].
- [44] B. A. Brown, Phys. Rev. Lett. **85**, 5296 (2000).
- [45] P. G. Reinhard, A. S. Umar, P. D. Stevenson, J. Piekarewicz, V. E. Oberacker, and J. A. Maruhn, Phys. Rev. C **93**, 044618 (2016), arXiv:1603.01319 [nucl-th].

- [46] C. Y. Tsang, B. A. Brown, F. J. Fattoyev, W. G. Lynch, and M. B. Tsang, *Phys. Rev. C* **100**, 062801 (2019), arXiv:1908.11842 [nucl-th].
- [47] C. Ducoin, J. Margueron, and C. Providencia, *EPL* **91**, 32001 (2010), arXiv:1004.5197 [nucl-th].
- [48] M. Fortin, C. Providencia, A. R. Raduta, F. Gulminelli, J. L. Zdunik, P. Haensel, and M. Bejger, *Phys. Rev. C* **94**, 035804 (2016), arXiv:1604.01944 [astro-ph.SR].
- [49] L.-W. Chen, C. M. Ko, B.-A. Li, and J. Xu, *Phys. Rev. C* **82**, 024321 (2010), arXiv:1004.4672 [nucl-th].
- [50] P. W. Zhao and S. Gandolfi, *Phys. Rev. C* **94**, 041302 (2016), arXiv:1604.01490 [nucl-th].
- [51] Z. Zhang, Y. Lim, J. W. Holt, and C. M. Ko, *Phys. Lett. B* **777**, 73 (2018), arXiv:1703.00866 [nucl-th].
- [52] Y. Wang, C. Guo, Q. Li, H. Zhang, Y. Leifels, and W. Trautmann, *Phys. Rev. C* **89**, 044603 (2014), arXiv:1403.7041 [nucl-th].
- [53] O. Lourenço, M. Bhuyan, C. H. Lenzi, M. Dutra, C. Gonzalez-Boquera, M. Centelles, and X. Viñas, *Phys. Lett. B* **803**, 135306 (2020), arXiv:2002.06242 [nucl-th].
- [54] M. Matsuzaki and M. Yahiro, (2022), arXiv:2207.00635 [nucl-th].
- [55] M. Matsuzaki, S. Tagami, and M. Yahiro, *Phys. Rev. C* **104**, 054613 (2021), arXiv:2107.06441 [nucl-th].
- [56] S. Tagami, T. Wakasa, M. Takechi, J. Matsui, and M. Yahiro, *Results in Physics* **33**, 105155 (2022).
- [57] B. T. Reed, F. J. Fattoyev, C. J. Horowitz, and J. Piekarewicz, *Phys. Rev. Lett.* **126**, 172503 (2021), arXiv:2101.03193 [nucl-th].

TABLE I. Properties of 207 EoSs (1). For the 207 EoSs, both $\Delta R_{\text{skin}}^{208}$ and L are obtained self-consistently; the starting $\Delta R_{\text{skin}}^{208}$ - L relation is determined from the EoSs in which both $\Delta R_{\text{skin}}^{208}$ and L are presented. For the 207 EoSs, we determine the relation between $\Delta R_{\text{skin}}^{208}$ and $\Delta R_{\text{skin}}^{48}$ self-consistently, where the starting $\Delta R_{\text{skin}}^{208}$ - $\Delta R_{\text{skin}}^{48}$ relation is determined from the EoSs in which both $\Delta R_{\text{skin}}^{208}$ and $\Delta R_{\text{skin}}^{48}$ are presented. The symbol † shows results of self-consistent calculations.

	m*/m	K	J	L	Ksym	Rskin-208	Rskin-48	Refs.
APR, E0019		266.000	32.600	57.600		0.160	0.160†	[30, 31, 44]
BHF-1		195.500	34.300	66.550	-31.300	0.200†	0.183†	[47]
BSk14	0.800	239.380	30.000	43.910	-152.030	0.164†	0.162†	[42, 47]
BSk16	0.800	241.730	30.000	34.870	-187.390	0.149†	0.154†	[42, 47]
BSk17	0.800	241.740	30.000	36.280	-181.860	0.151†	0.156†	[42, 47]
BSk20	0.800	241.400	30.000	37.400	-136.500	0.153†	0.157†	[42, 48]
BSk21	0.800	245.800	30.000	46.600	-37.200	0.168†	0.165†	[42, 48]
BSk22		245.900	32.000	68.500	13.000	0.204†	0.185†	[48]
BSk23		245.700	31.000	57.800	-11.300	0.186†	0.175†	[31, 48]
BSk24		245.500	30.000	46.400	-37.600	0.168†	0.165†	[48]
BSk25		236.000	29.000	36.900	-28.500	0.152†	0.156†	[48]
BSk26		240.800	30.000	37.500	-135.600	0.153†	0.157†	[48]
BSR2		239.900	31.500	62.000	-3.100	0.193†	0.179†	[48]
BSR6		235.800	35.600	85.700	-49.600	0.231†	0.200†	[48]
D1		229.400	30.700	18.360	-274.600	0.122†	0.139†	[34]
D1AS		229.400	31.300	66.550	-89.100	0.200†	0.183†	[34]
D1M	0.746‡	224.958‡	28.552‡	24.966‡	-133.692‡	0.113‡	0.147‡	[32]
D1M*	0.746‡	225.365‡	30.249‡	43.311‡	-47.793‡	0.134‡	0.158‡	[32]
D1MK	0.746‡	225.400‡	33.000‡	55.000‡	-37.275‡	0.158‡	0.171‡	[56]
D1N	0.748‡	225.525‡	29.594‡	33.665‡	-168.750‡	0.144‡	0.171‡	[32]
D1P	0.672‡	250.860‡	32.418‡	49.827‡	-157.419‡	0.179‡	0.157‡	[34]
D1PK	0.700‡	260.000‡	33.000‡	55.000‡	-150.000‡	0.182‡	0.181‡	[56]
D1S	0.697‡	202.856‡	31.125‡	22.558‡	-241.797‡	0.137‡	0.159‡	[32, 38]
D2	0.738	209.300	31.130	44.850		0.165†	0.163†	[32]
D250		249.900	31.570	24.820	-289.400	0.133†	0.145†	[34]
D260		259.500	30.110	17.570	-298.700	0.121†	0.139†	[34]
D280		285.200	33.140	46.530	-211.900	0.168†	0.165†	[34]
D300		299.100	31.220	25.840	-315.100	0.135†	0.146†	[34]
DD		241.000	31.700	56.000	-95.000	0.183†	0.173†	[49]
DD-F		223.000	31.600	56.000	-140.000	0.183†	0.173†	[49]
DD-ME1		245.000	33.100	55.000	-101.000	0.203†	0.193†	[31, 47, 49, 50]
DD-ME2		251.000	32.300	51.240	-87.000	0.203†	0.187†	[47-50]
DD-PC1				67.799		0.203†	0.195†	[47, 50]
Ducoin		240.200	32.760	55.300	-124.700	0.182†	0.173†	[47]
E0008(TMA)		318.000	30.660	90.140		0.239†	0.204†	[31]
E0009		280.000	32.500	88.700		0.236†	0.203†	[20, 31]
E0015		216.700	30.030	45.780		0.167	0.164	[31]
E0024		244.500	33.100	55.000		0.182†	0.172	[31]
E0025		211.000	31.600	107.400		0.267†	0.220†	[31]
E0036		281.000	36.900	110.800		0.272†	0.223†	[31]
es25		211.730	25.000	27.749†		0.138	0.148†	[40]
es275		205.330	27.500	48.549†		0.171	0.167†	[40, 48]
es30		215.360	30.000	69.603†		0.205	0.186†	[40]
es325		212.450	32.500	81.925†		0.225	0.197†	[40]
es35		209.970	34.937	96.182†		0.248	0.210†	[40]
FKVW		379.000	33.100	80.000	11.000	0.222†	0.195†	[49]
FSU		230.000	32.590	60.500	-51.300	0.210	0.188†	[39, 47]
FSUgold		229.000	32.500	60.000	-52.000	0.210	0.200	[20, 35, 49]
FSUgold2.1		230.000	32.590	60.500		0.191†	0.177†	[20, 31]
GM1		299.700	32.480	93.870	17.890	0.245†	0.207†	[47, 48]
GM3		239.900	32.480	89.660	-6.470	0.238†	0.204†	[47]
Gs		237.570	31.384	89.304†		0.237	0.203†	[40]
GSkI		230.210	32.030	63.450	-95.290	0.195†	0.180†	[42]
GSkII	0.790	233.400	30.490	48.630	-157.830	0.171†	0.167†	[42]
GT2		228.100	33.940	5.020	-445.900	0.101†	0.127†	[34]
Gσ		237.290	31.370	94.020	13.990	0.245†	0.208†	[47]
HA		233.000	30.700	55.000	-135.000	0.182†	0.172†	[49]
HFB-17				36.300		0.151	0.155†	[24]
HFB-8				14.800		0.115	0.135†	[24]
HS(DD2)		243.000	31.700	55.000	-93.200	0.182†	0.172†	[20, 48]
IU-FSU		231.200	31.300	47.200	28.700	0.160	0.160†	[20, 39]
KDE0v1	0.740	227.540	34.580	54.690	-127.120	0.181†	0.172†	[42]
KDE0v1-B	0.790	216.000	34.900	61.000		0.192	0.172	[43]

TABLE I. Properties of 207 EoSs (2).

	m^*/m	K	J	L	Ksym	Rskin-208	Rskin-48	Refs.
KDE0v1-T	0.810	217.000	34.600	72.000	-40.000	0.200	0.178	[46]
LNS	0.830	210.780	33.430	61.450	-127.360	0.192 [†]	0.178 [†]	[42, 47]
LS180		180.000	28.600	73.800		0.212 [†]	0.189 [†]	[20, 31, 42]
LS220		220.000	28.600	73.800		0.212 [†]	0.189 [†]	[20, 31, 42]
LS375		375.000	28.600	73.800		0.212 [†]	0.189 [†]	[20, 31, 42]
Ly5		229.940	32.010	45.243 [†]		0.166	0.164 [†]	[40]
M3Y-P6		239.700	32.100	44.600	-165.300	0.165 [†]	0.163 [†]	[36, 38]
M3Y-P7		254.700	31.700	51.500	-127.800	0.176 [†]	0.169 [†]	[38, 48]
MSK3	1.000	233.250	28.000	7.040	-283.520	0.111	0.128	[42, 50]
MSK6	1.050	231.170	28.000	9.630	-274.330	0.118	0.130	[42, 50]
MSK7	1.050	385.360	27.950	9.400	-274.630	0.116	0.136 [†]	[24, 42]
MSL0	0.800	230.000	30.000	60.000	-99.330	0.180	0.171 [†]	[42, 49, 52]
NL1		212.000	43.500	140.000	143.000	0.319	0.247	[49, 50]
NL2		401.000	44.000	130.000	20.000	0.304	0.243	[49, 50]
NL3		271.000	37.300	118.000	100.000	0.280	0.230	[35, 39, 41, 47–49]
NL3*				119.769 [†]		0.287	0.230	[50]
NL3 $\omega\rho$		271.600	31.700	55.500	-7.600	0.183 [†]	0.173 [†]	[48]
NL4		270.350	36.239	111.649 [†]		0.273	0.223 [†]	[40]
NL-SH		356.000	36.100	114.000	80.000	0.263	0.214	[49, 50]
NL ρ		240.000	30.300	85.000	3.000	0.230 [†]	0.199 [†]	[49]
NL $\omega\rho(025)$		270.700	32.350	61.050	-34.360	0.192 [†]	0.178 [†]	[47]
NRAPR	0.690	225.700	32.787	59.630	-123.320	0.190	0.177 [†]	[40, 42]
NRAPR-B	0.850	225.000	35.100	61.000		0.193	0.178	[43]
NRAPR-T	0.730	221.000	34.100	70.000	-46.000	0.195	0.181	[46]
PC-F1		255.000	37.800	117.000	75.000	0.269	0.225	[49, 50]
PC-F2		256.000	37.600	116.000	65.000	0.281 [†]	0.227 [†]	[49, 50, 52]
PC-F3		256.000	38.300	119.000	74.000	0.285 [†]	0.230 [†]	[49, 50]
PC-F4		255.000	37.700	119.000	98.000	0.285 [†]	0.230 [†]	[49]
PC-LA		263.000	37.200	108.000	-61.000	0.268 [†]	0.220 [†]	[49]
PC-PK1				101.478		0.257	0.220	[50]
PK1		282.000	37.600	116.000	55.000	0.277	0.223	[49, 50]
PKDD		263.000	36.900	90.000	-80.000	0.253	0.214	[49, 50]
RAPR		276.700	33.987	66.958 [†]		0.201	0.183 [†]	[40]
RATP		239.580	29.260	32.390	-191.250	0.145 [†]	0.152 [†]	[47]
rDD-ME2				51.300		0.193	0.179 [†]	[24]
rFSUGold				60.500		0.207	0.186 [†]	[24, 48]
rG2				100.700		0.257	0.214 [†]	[24]
rNL1				140.100		0.321	0.250 [†]	[24]
rNL3				118.500		0.280	0.227 [†]	[24]
rNL3*				122.600		0.288	0.232 [†]	[24]
rNLC				108.000		0.263	0.218 [†]	[24]
rNL-RA1				115.400		0.274	0.224 [†]	[24]
rNL-SH				113.600		0.266	0.219 [†]	[24]
rNL-Z				133.300		0.307	0.242 [†]	[24]
Rs		237.660	30.593	80.096 [†]	-9.100	0.222	0.195 [†]	[40, 48]
rTM1				110.800		0.271	0.222 [†]	[24]
R σ		237.410	30.580	85.700	-9.130	0.231 [†]	0.200 [†]	[47]
S271		271.000	35.927	97.541 [†]		0.251	0.211 [†]	[40]
SFHo		245.000	31.600	47.100		0.169 [†]	0.165 [†]	[20]
SFHx		239.000	28.700	23.200		0.130 [†]	0.144 [†]	[20]
SGI	0.610	262.000	28.300	63.900	-51.990	0.196 [†]	0.180 [†]	[36, 40, 42]
SGII	0.790	214.700	26.830	37.620	-145.920	0.136	0.147 [†]	[24, 38, 42, 47]
SII	0.580	341.400	34.160	50.020	-265.720	0.196	0.177	[50]
SIII	0.760	355.37	28.160	9.910	-393.730	0.137	0.125	[42, 50]
Sk χ m		230.400	30.940	45.600		0.167	0.164 [†]	[42, 51]
SK255		254.960	37.400	95.000	-58.300	0.247 [†]	0.208 [†]	[48]
SK272		271.550	37.400	91.700	-67.800	0.241 [†]	0.205 [†]	[48]
Ska	0.610	263.160	32.910	74.620	-78.460	0.214 [†]	0.190 [†]	[20, 24, 38, 42, 48, 52]
Ska25-B	0.990	219.000	32.500	51.000		0.176	0.170	[43]
Ska25s20	0.980	220.750	33.780	63.810	-118.220	0.196 [†]	0.180 [†]	[42]
Ska25-T	0.980	220.000	31.900	59.000	-59.000	0.183	0.176	[46]
Ska35-B	1.000	244.000	32.800	54.000		0.180	0.172	[43]
Ska35s20	1.000	240.270	33.570	64.830	-120.320	0.198 [†]	0.181 [†]	[42, 52]
Ska35-T	0.990	238.000	32.000	58.000	-84.000	0.184	0.177	[42, 46, 47]

TABLE I. Properties of 207 EoSs (3).

	m*/m	K	J	L	Ksym	Rskin-208	Rskin-48	Refs.
SKb	0.610	263.000	33.880	47.600	-78.500	0.170 [†]	0.166 [†]	[42, 48]
SkI1	0.690	242.750	37.530	161.050	234.670	0.353 [†]	0.268 [†]	[42, 52]
SkI2	0.680	240.700	33.400	104.300	70.600	0.262 [†]	0.217 [†]	[38, 42, 47, 48]
SkI3	0.580	258.000	34.800	100.500	72.900	0.255 [†]	0.213 [†]	[38, 42, 47, 48]
SkI4	0.650	247.700	29.500	60.400	-40.600	0.191 [†]	0.177 [†]	[36, 38, 42, 47, 48]
SkI5	0.580	255.800	36.697	129.300	159.500	0.272	0.214	[38, 40, 42, 47, 48]
SkI6	0.640	248.650	30.090	59.700	-47.270	0.189 [†]	0.177 [†]	[42, 47, 48]
SkM*	0.790	216.610	30.030	45.780	-155.940	0.170	0.155	[24, 38, 42, 50]
SkM*-B	0.780	218.000	34.200	58.000		0.187	0.175	[43]
SkM*-T	0.790	219.000	33.700	65.000	-65.000	0.187	0.179	[46?]
SkMP	0.650	230.930	29.890	70.310	-49.820	0.197	0.167	[24, 47? , 48]
SkO	0.900	223.390	31.970	79.140	-43.170	0.221 [†]	0.194 [†]	[42, 47]
SKOp	0.900	222.360	31.950	68.940	-78.820	0.204 [†]	0.185 [†]	[42, 48]
SKP	1.000	200.970	30.000	19.680	-266.600	0.144	0.144	[42, 50]
SKRA	0.750	216.980	31.320	53.040	-139.280	0.179 [†]	0.171 [†]	[42]
SKRA-B	0.790	212.000	33.700	55.000		0.181	0.172	[42, 43]
SKRA-T	0.800	213.000	33.400	65.000	-55.000	0.190	0.179	[42, 46]
Sk-Rs				85.700		0.215	0.191 [†]	[24]
SkSM*				65.500		0.197	0.181 [†]	[24]
SKT1	1.000	236.160	32.020	56.180	-134.830	0.184 [†]	0.173 [†]	[42]
SKT1-B	0.970	242.000	33.300	56.000		0.183	0.172	[43]
SKT1-T	0.970	238.000	32.600	63.000	-70.000	0.190	0.179	[42, 46]
SKT2	1.000	235.730	32.000	56.160	-134.670	0.184 [†]	0.173 [†]	[42]
SKT2-B	0.970	242.000	33.500	58.000		0.186	0.174	[43]
SKT2-T	0.960	238.000	32.600	62.000	-75.000	0.188	0.178	[42, 46]
SKT3	1.000	235.740	31.500	55.310	-132.050	0.182 [†]	0.173 [†]	[42]
SKT3-B	0.980	241.000	32.700	53.000		0.179	0.172	[43]
SKT3-T	0.970	236.000	31.900	58.000	-80.000	0.183	0.178	[46]
Sk-T4	1.000	235.560	35.457	94.100	-24.500	0.253	0.212 [†]	[24, 38, 40]
Sk-T6	1.000	235.950	29.970	30.900	-211.530	0.151	0.155 [†]	[24, 42]
Skxs20	0.960	201.950	35.500	67.060	-122.310	0.201 [†]	0.183 [†]	[42]
Skz2	0.700	230.070	32.010	16.810	-259.660	0.120 [†]	0.138 [†]	[42, 52]
Skz4	0.700	230.080	32.010	5.750	-240.860	0.102 [†]	0.128 [†]	[42, 52]
SLy0	0.700	229.670	31.982	44.873 [†]	-116.230	0.165	0.163 [†]	[40, 42]
SLy10	0.680	229.740	31.980	38.740	-142.190	0.155 [†]	0.158 [†]	[42, 47]
Sly2	0.700	229.920	32.000	47.460	-115.130	0.170 [†]	0.166 [†]	[42, 48]
SLy230a	0.700	229.890	31.980	44.310	-98.210	0.155	0.158 [†]	[40, 42, 47, 48]
Sly230b	0.690	229.960	32.010	45.960	-119.720	0.167 [†]	0.164 [†]	[42, 47]
SLy4	0.690	229.900	32.000	45.900	-119.700	0.162	0.152	[24, 32, 36, 38, 48, 50]
SLy4-B	0.700	224.000	34.100	56.000		0.184	0.174	[43]
SLy4-T	0.760	222.000	33.600	66.000	-55.000	0.191	0.179	[42, 46]
SLy5	0.700	229.920	32.010	48.150	-112.760	0.162	0.160	[42, 50]
SLy6	0.690	229.860	31.960	47.450	-112.710	0.161	0.152	[42, 50]
Sly9	0.670	229.840	31.980	54.860	-81.420	0.182 [†]	0.172 [†]	[42, 48]
SQMC650	0.780	218.110	33.650	52.920	-173.150	0.178 [†]	0.171 [†]	[42]
SQMC700	0.760	222.200	33.470	59.060	-140.840	0.188 [†]	0.176 [†]	[42]
SQMC750-B	0.710	228.000	34.800	59.000		0.190	0.176	[43]
SQMC750-T	0.750	223.000	33.900	68.000	-50.000	0.194	0.180	[42, 46]
SR1	0.900	202.150	29.000	41.245 [†]		0.160	0.160 [†]	[40]
SR2		224.640	30.071	49.130 [†]		0.172	0.167 [†]	[40]
SR3		222.550	29.001	48.308 [†]		0.171	0.166 [†]	[40]
SV	0.380	306.000	32.800	96.100	24.190	0.230	0.196	[36, 42, 47, 50]
SV-bas	0.900	221.760	30.000	32.000	-156.570	0.155	0.158 [†]	[42, 45]
SV-K218	0.900	218.230	30.000	35.000	-207.870	0.161	0.161 [†]	[42, 45]
SV-K226	0.900	225.820	30.000	34.000	-211.920	0.159	0.160 [†]	[42, 45]
SV-K241	0.900	241.070	30.000	31.000	-230.770	0.151	0.155 [†]	[42, 45]
SV-kap00	0.900	233.440	30.000	40.000	-161.780	0.158	0.159 [†]	[42, 45]
SV-kap20	0.900	233.440	30.000	36.000	-193.190	0.155	0.158 [†]	[42, 45]
SV-kap60	0.900	233.450	30.000	29.000	-249.750	0.154	0.157 [†]	[42, 45]
SV-L25	0.900		30.000	25.000		0.143	0.151 [†]	[45]
SV-L32	0.900		30.000	32.000		0.154	0.157 [†]	[45]
SV-L40	0.900	233.3	30.000	40.000		0.166	0.164 [†]	[45]
SV-L47	0.900	233.4	30.000	47.000		0.177	0.170 [†]	[45]

TABLE I. Properties of 207 EoSs (4).

	m*/m	K	J	L	Ksym	Rskin-208	Rskin-48	Refs.
SV-mas07	0.700	233.540	30.000	52.000	-98.770	0.152	0.156 [†]	[42, 45]
SV-mas08	0.800	233.130	30.000	40.000	-172.380	0.160	0.160 [†]	[42, 45, 52]
SV-mas10	1.000	234.330	30.000	28.000	-252.500	0.152	0.156 [†]	[42, 45]
SV-sym28	0.900	240.860	28.000	7.000	-305.940	0.117	0.136 [†]	[42, 45]
SV-sym32	0.900	233.810	32.000	57.000	-148.790	0.192	0.178 [†]	[42, 45]
SV-sym32-B	0.910	237.000	32.300	51.000		0.176	0.174	[43]
SV-sym32-T	0.910	232.000	31.500	58.000	-77.000	0.181	0.179	[46]
SV-sym34	0.900	234.070	34.000	81.000	-79.080	0.227	0.198 [†]	[42, 45, 52]
TFa		245.100	35.050	82.500	-68.400	0.250	0.210 [†]	[39]
TFb		250.100	40.070	122.500	45.800	0.300	0.238 [†]	[39]
TFc		260.500	43.670	135.200	51.600	0.330	0.255 [†]	[39]
TM1		281.000	36.900	110.800	33.550	0.272 [†]	0.223 [†]	[31, 47–49]
TW99		241.000	32.800	55.000	-124.000	0.196	0.186	[49, 50]
UNEDF0		229.800	30.500	45.100	-189.600	0.166 [†]	0.164 [†]	[38, 42]
UNEDF1		219.800	29.000	40.000	-179.400	0.158 [†]	0.159 [†]	[38]
Z271		271.000	35.369	89.520 [†]		0.238	0.204 [†]	[40]
Sly7				45.900		0.150	0.153	[54, 55]